Hyon *et al.*
Journal of Analytical Science and Technology (2023) 14:1
https://doi.org/10.1186/s40543-022-00365-y

Journal of Analytical Science and Technology

RESEARCH ARTICLE

Open Access

Comparative proteomics study of mitochondrial electron transport system modulation in SH-SY5Y cells following MPP+ versus 6-OHDA-induced neurodegeneration

Ju-Yong Hyon[1†], Hea Ji Lee[1,2†], Sung Ho Yun[3], Eun Hee Han[1,4] and Young-Ho Chung[1,2*]

Abstract

Parkinson's disease (PD) is the second-most common neurodegenerative disease worldwide. Several studies have investigated PD for decades; however, the exact mechanism of disease development remains unknown. To study PD, SH-SY5Y cells are often treated with 6-hydroxydopamine (6-OHDA) or 1-methyl-4-phenylpyridinium (MPP+) to induce PD. To understand the mechanism of PD pathogenesis, we confirmed protein changes between 6-OHDA- and MPP+-treated SH-SY5Y cells via proteomics analysis using liquid chromatography coupled with tandem mass spectrometry. 6-OHDA-treated SH-SY5Y cells showed increased expression of electron transporter-related proteins compared to that in the control group, along with decreased expression in MPP+-treated SH-SY5Y cells. However, both down- and upregulation of electron transporter-related proteins increased mitochondrial dysfunction and apoptosis. These proteins were confirmed via protein–protein interaction network analysis using IPA and STRING to induce mitochondrial dysfunction and apoptosis. Cell-based experiments using flow cytometry verified that apoptosis and mitochondrial membrane potential were increased in both 6-OHDA- and MPP+-treated SH-SY5Y cells. Our results provide new insights into PD pathogenesis, thereby contributing to the understanding of the mechanisms of PD development.

Keywords Parkinson's disease, 6-Hydroxydopamine, 1-Methyl-4-phenylpyridinium, Mitochondrial dysfunction, Liquid chromatography–tandem mass spectrometry

Introduction

Parkinson's disease (PD) is a representative neurodegenerative disease caused by the progressive loss of cellular structure or function, including the death of neuronal cells. The exact mechanism of neuronal cell death in neurodegeneration has not been fully elucidated; however, it is mostly accompanied by increased protein aggregation (Bence et al. 2001; Muchowski and Wacker 2005) and oxidative stress (Tsang and Chung 2009). Human neuroblastoma SH-SY5Y cells represent a well-characterized cell-based model of dopaminergic neurons, and these cells show intermediate activity of important neuronal markers commonly present in dopaminergic cells, such as noradrenaline (Kovalevich and Langford 2013), choline acetyltransferase (Filograna et al. 2015), tyrosine

†Ju-Yong Hyon and Hea Ji Lee contributed equally to this work

*Correspondence:
Young-Ho Chung
chungyh@kbsi.re.kr
[1] Research Center for Bioconvergence Analysis, Korea Basic Science Institute (KBSI), Cheongju, Chungbuk 28119, Republic of Korea
[2] Department of Analytical Science and Technology, Graduate School of Analytical Science and Technology (GRAST), Chungnam National University, Daejeon 34134, Republic of Korea
[3] Center for Research Equipment, Korea Basic Science Institute (KBSI), Cheongju, Chungbuk 28119, Republic of Korea
[4] Department of Bio-Analytical Science, University of Science and Technology (UST), Daejeon 34113, Republic of Korea

hydroxylase (Khwanraj et al. 2015), and dopamine-β-hydroxylase (Katsuyama et al. 2021). Consequently, SH-SY5Y cells have long been used in PD research to explore the underlying cellular and molecular mechanisms of neurodegeneration.

The toxin, 6-hydroxydopamine (6-OHDA) is commonly used to induce degeneration of dopaminergic neurons in PD (Blum et al. 2001). It increases the production of reactive oxygen species (ROS), which disrupt complex I of the mitochondrial electron transfer chain and contribute to apoptotic cell death. Similar to 6-OHDA, 1-Methyl-4-phenylpyridinium (MPP+), the oxidized product of 1-methyl-4-phenyl-1,2,3,6-tetrahydropyridine (MPTP) decreases mitochondrial activity and increases ROS generation in neuronal cells (Perfeito et al. 2013). However, the mechanism underlying 6-OHDA- and MPP+-induced injury remains unclear. Previous studies have only reported the effects of 6-OHDA and MPP+ on neuronal cells separately (Blum et al. 2001; Perfeito et al. 2013; Xie et al. 2011; Komatsubara et al. 2012; Choi et al. 2014; Alberio et al. 2014; Magalingam et al. 2022), and none of them have directly compared the effects of 6-OHDA and MPP+ on neuronal cells. Thus, large-scale proteome investigation of the effects of 6-OHDA and MPP+ on neuronal cells will bring new insights into PD.

Proteomics research using liquid chromatography–tandem mass spectrometry (LC–MS/MS) involves large-scale protein expression analysis that provides biological insights into cellular structures and functions. Because of the advantage of analyzing large-scale protein expression, proteomics research for PD is being actively conducted (Xie et al. 2011; Komatsubara et al. 2012; Choi et al. 2014; Alberio et al. 2014; Magalingam et al. 2022). Proteins within the cell play a crucial role in providing cellular structure, movement, and communication, and participate in metabolism, respiration, signal transduction, and reproduction activities. Intracellular proteins similarly play an important role in cellular structure, movement, and communication, and also participate in various metabolic activities and signaling (Aslam et al. 2017). Thus, changes in protein expression/differentially expressed proteins (DEPs) represent important signals of changes in cell activity.

In the present study, we performed label-free global protein profiling of a PD cell model using 6-OHDA- or MPP+-induced neurodegeneration of SH-SY5Y cells based on a shotgun proteomic methodology. The main purpose of this study was to compare and analyze the similarities and differences between 6 and OHDA- and MPP+-induced PD models via proteomic analysis to understand the pathogenesis of PD and identify novel therapeutic targets or biomarkers of PD.

Methods

Cell culture and treatment with 6-OHDA or MPP+

SH-SY5Y cells were purchased from the Korean Cell Line Bank (Seoul, Korea) and grown in high-glucose Dulbecco's modified Eagle medium (DMEM; Hyclone, San Angelo, TX, USA) supplemented with 10% fetal bovine serum (FBS; Hyclone) and 1% penicillin/streptomycin (Hyclone) at 37 °C in a humidified atmosphere with 5% CO_2. The cells were transferred to another cell culture dish every 3 days and maintained. The SH-SY5Y cells were seeded for 24 h and treated with the newly prepared 6-OHDA at the indicated concentration for 48 h with 10% FBS; in the case of MPP+, 5% FBS was used in the same manner (Do Lee et al. 2008).

Cell viability

For measuring cell viability, SH-SY5Y cells were seeded at a density of 5×10^3 cells/mL in a 96-well plate and incubated at 37 °C in CO_2 for 24 h. Cells were treated with different concentrations of 6-OHDA or MPP+ and then incubated at 37 °C with CO_2. After 48 h, the Cell Counting Kit-8 (CCK-8; Dojindo Molecular Technologies, Inc., Rockville, MD, USA) was added to the cells in a 96-well plate following incubation for 1 h. The cell viability of the treated cells was determined after measuring the absorbance at 450 nm using SpectroMax M4 (Molecular Devices, San Jose, CA, USA).

Quantitative real-time polymerase chain reaction (PCR)

Total RNA was extracted from SH-SY5Y cells using an RNeasy Mini Kit (Qiagen, Hilden, Germany), and 1 μg of RNA was reverse-transcribed to cDNA using the EcoDry Premix (Double Primed; TaKaRa Bio, Kusatsu, Japan) and then amplified via PCR. Product formation was monitored continuously during PCR using the Sequence Detection QuantStudio 3 Real-Time PCR System (Applied Biosystems, Waltham, MA, USA). Accumulated PCR products were detected directly by monitoring the increase in reporter dye (SYBR) signal. Expression levels of synuclein alpha (*SNCA*) (forward 5′-TGACAAATG TTGGAGGAGCA-3′, reverse 5′-TGTCAGGATCCA CAGGCATA-3′), leucine-rich repeat kinase 2 (*LRRK2*) (forward 5′-ATGTCATGCTGGTATTGGGCT-3′, reverse 5′-GTCCCAAACGGTCAAGCAAG-3′), parkin (forward 5′-CTGACACCAGCATCTTCCAG-3′, reverse 5′-CCAGTCATTCCTCAGCTCCT-3′), and β-actin (forward 5′-CATGTACGTTGCTATCCAGGC-3′, reverse 5′-CTCCTTATGTCACGCCACGAT-3′) in treated cells were compared with those in control cells using the comparative cycle threshold method.

Preparation of protein samples

Proteins were isolated from SH-SY5Y cells, which were treated with or without 6-OHDA or MPP+, in NETN lysis buffer containing a proteinase inhibitor and phosphatase inhibitor cocktail (Invitrogen, Waltham, MA, USA). Protein concentration was measured using a BCA protein assay kit (Thermo Fisher Scientific, Waltham, MA, USA).

In-gel digestion and proteomics analysis using LC–MS/MS

Proteins (40 μg) were loaded in sodium dodecyl sulfate–polyacrylamide gels and subjected to in-gel digestion for proteome analysis, as described previously (Lee et al. 2021a). Each proteome was tryptic-digested and analyzed via LC–MS/MS using an Ultimate 3000 RSLCnano system (Thermo Fisher Scientific, Bremen, Germany) coupled with a Q-Exactive Plus mass spectrometer (Thermo Fisher Scientific, Bremen, Germany) via nano-electrospray as described in our previous study (Lee et al. 2021b). Briefly, the peptide samples were separated on a two-column system with a trap column (300 μm I.D × 5 mm) and an analytical column (75 μm I.D × 50 cm) with a 120 min gradient from 6 to 30% acetonitrile. Mass spectra were acquired in data-dependent mode with MS1 scans at a 60,000 resolution at m/z 200. The top 20 ions with an isolation window of 2 m/z were selected and fragmented using HCD with normalized collision energy of 28. The maximum ion injection times for the MS1 and MS2 scans were 25 and 125 ms, respectively.

Data processing

MS raw files were processed using MaxQuant version 2.1.4 (Matrix Science, Chicago, IL, USA) with the Andromeda search engine against the UniProt human protein database reference proteome database, including forward and reverse sequences and common contaminants (Cox and Mann 2008; Cox et al. 2011). To quantitatively compare protein abundance in each sample, DEPs were calculated using the label-free quantification (LFQ) value. Low-confidence peptides were filtered using a false discovery rate of at least 1% using a target-decoy search strategy. To ensure fidelity, proteins that were identified more than twice in three replicates were considered valid. For comparative analysis, the LFQ value was normalized by log2 transformation, and the missing values were imputed assuming a normal distribution (Bertin et al. 2013; Välikangas et al. 2018). DEPs were selected using the significance analysis of the microarray method (Tusher et al. 2001), modifying the gene-specific t-statistic calculated via repeated permutation with the background. DEPs were analyzed using core analysis of the Ingenuity Pathway Analysis (IPA, version 68752261) to gain biological insight into the data.

Pathway enrichment analysis

Pathway enrichment analysis of the DEPs was performed using the Metascape bioinformatics online database (https://metascape.org/) (Zhou et al. 2019). The cluster with the most enriched proteins exhibiting strong protein–protein interaction (PPI) was identified using STRING (https://string-db.org/) analysis. The enriched pathway curated by Kyoto Encyclopedia of Genes and Genomes (KEGG; https://www.kegg.jp/kegg/mapper/color.html) was used to elucidate the molecular mechanisms of the DEPs.

Apoptosis analysis

Apoptosis was evaluated using an Annexin V and propidium iodide (PI) flow cytometry kit (Invitrogen, V13242) according to the manufacturer's instructions. SH-SY5Y cells were treated with 6-OHDA (50 μM) or MPP+ (500 μM) for 48 h. Subsequently, the cells were harvested via centrifugation, washed once with a buffer containing 10 mM HEPES, 140 mM NaCl, 2.5 mM $CaCl_2$, and stained with Annexin V-fluorescein isothiocyanate (FITC) and PI in the dark at room temperature (25–28 °C) for 15 min. Finally, the cells were analyzed using flow cytometry (CytoFlex; Beckman Coulter, Brea, CA, USA).

Measurement of mitochondrial membrane potential (MMP)

MMP was measured using JC-1 dye (5′,6,6′-tetrachloro-1,1′,3,3′-tetraethylbenzimidazolylcarbocyanine iodide; Life Technologies, Carlsbad, CA, USA) according to the manufacturer's instructions. Briefly, 6-OHDA- or MPP+-treated cells were incubated with 10 μg/mL JC-1 dye for 15 min, and the fluorescence intensity was measured using a CytoFlex instrument (Beckman Coulter). JC-1 aggregates (high $\Delta\psi M$) were in the PE channel and monomers (low $\Delta\psi M$) were in the FITC channel.

Statistical analysis

All data are presented as the mean ± standard deviation. Statistical analysis was performed using a two-tailed Student's t test using the GraphPad Prism 5 analysis package (GraphPad Software, San Diego, CA, USA) and Perseus software (Tyanova et al. 2016). Statistical significance was set at $p < 0.05$. All data were obtained from at least three independent experiments.

Results and discussion

Development of in vitro PD model of SH-SY5Y cells treated with 6-OHDA or MPP+

An in vitro PD model can be established by treating SH-SY5Y cells with 6-OHDA or MPP+. PD model cells exhibit mitochondrial dysfunction and apoptotic features (Blum et al. 2001; Do Lee et al. 2008). We confirmed that PD-related gene expression, cell apoptosis, and mitochondrial dysfunction increased based on qRT-PCR and fluorescence-activated cell sorting (FACS) experiments

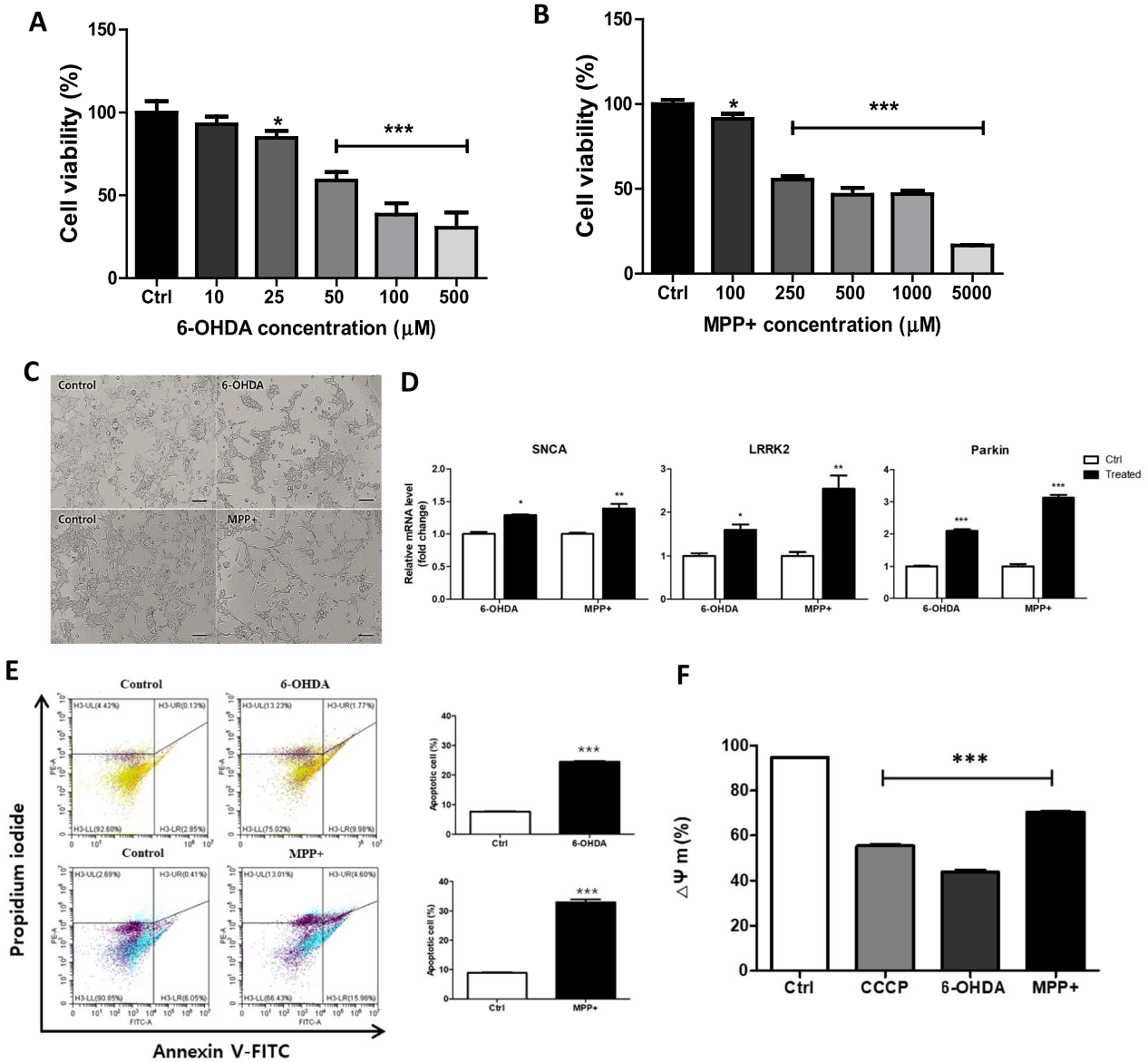

Fig. 1 In vitro model validation of Parkinson's disease for SH-SY5Y cells treated with 6-OHDA or MPP+. SH-SY5Y cells were treated with different concentrations of **A** 6-OHDA (0, 10, 25, 50, 100, and 500 μM) or **B** MPP+ (0, 100, 250, 500, 1000, and 5000 μM) for 48 h; cell viability was analyzed using Cell Counting Kit-8. **C** Cellular morphology changes caused by 50 μM 6-OHDA and 500 μM MPP+ (Scale bar = 100 μm). **D** The expression of PD-related genes, including *SNCA*, *LRRK2*, and parkin, was confirmed in 6-OHDA or MPP+-treated SH-SY5Y cells using qRT-PCR. The β-actin transcript served as an internal control. Apoptosis was quantified via FACS after Annexin V-FITC and PI labeling. Representative FACS data are shown for SH-SY5Y cells treated with 6-OHDA and MPP+ under normal and low fetal bovine serum (5%) conditions. The abscissa and ordinate represent the fluorescence intensity of Annexin V-FITC and PI, respectively. **E** The bar graph represents the level of apoptosis. **F** Cells were treated with 6-OHDA or MPP+ for 48 h, and the mitochondrial membrane potential (ΔψM) was measured based on JC-1 fluorescence via flow cytometry. (***$p < 0.001$, **$p < 0.01$, *$p < 0.05$, $n = 3$). *6-OHDA* 6-hydroxydopamine, *MPP+* 1-methyl-4-phenylpyridinium; *Ctrl* control, *FITC* fluorescein isothiocyanate, *PI* propidium iodide

on 6-OHDA- and MPP+-treated SH-SY5Y cells to verify an in vitro PD model using SH-SY5Y cells. First, cytotoxicity was confirmed by treating the cells with 6-OHDA or MPP+ at various concentrations. 6-OHDA was toxic at 25 μM, and MPP+ was toxic at 100 μM (Fig. 1A, B). Based on these findings, subsequent experiments used 6-OHDA (50 μM) and MPP+ (500 μM) with a concentration associated with approximately 50% cell survival. This is similar to the treatment concentrations of 6-OHDA (Zhang et al. 2014) and MPP+ (Wang et al. 2018) used in previous studies. The morphology of SH-SY5Y cells treated with 50 μM 6-OHDA and 500 μM MPP+ was altered (Fig. 1C). To determine whether 6-OHDA- and MPP+-treated SH-SY5Y cells exhibited PD characteristics, the expression of *SNCA*, *LRRK2*, and parkin genes, known as PD biomarkers (Ross et al. 2008; Wang and Song 2016; Smith et al. 2005), was evaluated using qRT-PCR; the expression level of each gene was increased in 6-OHDA- and MPP+-treated SH-SY5Y cells (Fig. 1D). Finally, FACS experiments confirmed that mitochondrial dysfunction and apoptosis were increased in 6-OHDA- and MPP+-treated SH-SY5Y cells (Fig. 1E, F), as reported in previous studies (Wang et al. 2014; Chen et al. 2021; Ganapathy et al. 2016). These results indicate that neurodegeneration was induced in 6-OHDA- and MPP+-treated SH-SY5Y cells that simulated PD.

Identification and quantification of DEPs using label-free mass spectrometry

The protein profiling of 6-OHDA-induced neurodegeneration versus untreated SH-SY5Y cells and MPP+-induced neurodegeneration versus untreated SH-SY5Y cells were analyzed using MaxQuant software. Label-free MS/MS identified 3798 and 4078 proteins in the 6-OHDA-treated and untreated SH-SY5Y cells, respectively, and 3532 and 3837 proteins in the MPP+-treated and untreated SH-SY5Y cells, respectively. Approximately 3016 proteins in SH-SY5Y cells treated with 6-OHDA or MPP+ and in untreated SH-SY5Y cells were identified at least twice in biological triplicates (Fig. 2A).

Among the 3016 commonly identified proteins mentioned above, a protein comparison between untreated and 6-OHDA-treated SH-SY5Y cells revealed that a total of 461 proteins had a significant difference in expression ($p < 0.05$). Among them, 38 upregulated and 16 downregulated proteins showing differences in DEP > 1 were identified via Log2 fold-change distribution (Fig. 2B). When comparing proteins between MPP+-treated and untreated SH-SY5Y cells among the 3016 commonly identified proteins, 1465 proteins showing significant differences in expression ($p < 0.05$) were identified. Among these 1465 proteins, 172 upregulated proteins and 364 downregulated proteins showing differences in DEP > 1 were identified via Log2 fold-change distribution (Fig. 2C).

Bioinformatics analysis of DEPs

To further elucidate the neurodegeneration process in SH-SY5Y cells induced by 6-OHDA and MPP+, we used the Metascape bioinformatics database (Zhou et al. 2019) to analyze the gene ontology (GO) and reactome gene sets of 461 and 1465 DEPs ($p < 0.05$) in 6-OHDA- and MPP+-treated SH-SY5Y cells. These proteins were analyzed based on changes in the biological processes of the GO term classification cluster. According to GO biological process analysis, upregulated proteins in 6-OHDA-treated SH-SY5Y cells respond to external stress, and as previous studies have shown (Magalingam et al. 2022), proteins that regulate ribosomal assembly were upregulated. These results were consistent with reactome gene set analysis (Fig. 3A, upper panel). Conversely, the protein downregulation by 6-OHDA treatment was found to induce mitochondrial dysfunction and an imbalance in metabolic processes based on GO biological process analysis, and the tricarboxylic acid (TCA) cycle and respiratory electron transport protein expression were suppressed based on reactome gene set analysis (Fig. 3A, lower panel). In addition, IPA network analysis showed that heat shock protein 60 member 1 (HSPD1) induced a decrease in ATPase expression (Fig. 3C). HSPD1 is a member of the folding/trapping group and is categorized as a protein that helps fold, transport, and localize proteins. HSPD1 interacts with various proteins and can considerably affect SNCA biosynthesis and pathological properties (Hernandez et al. 2020). These results suggest that 6-OHDA-induced neurodegeneration in SH-SY5Y cells may be induced by mitochondrial dysfunction by disrupting the TCA cycle and electron transport system. The results of our study suggest that mitochondrial dysfunction is induced by disruption of the TCA cycle and electron transport system and may provide clues to further explore the underlying causes of mitochondrial dysfunction in PD.

Based on the GO biological process and reactome gene set analysis of MPP+-treated SH-SY5Y cells, the proteins upregulated by MPP+ treatment in response to external stress were consistent with those observed after 6-OHDA treatment; however, proteins associated with apoptosis were upregulated (Fig. 3B, upper panel). Proteins downregulated by MPP+ treatment were mainly found to be reduced in DNA synthesis, RNA synthesis, and cell cycle-related proteins (Fig. 3B, lower panel). IPA network analysis of 1465 proteins significantly altered by MPP+ in SH-SY5Y cells showed that MPP+ inhibited β-hydroxy β-methylglutaryl-CoA (HMG-CoA) synthesis via β-catenin (CTNNB1) protein. CTNNB1 is a

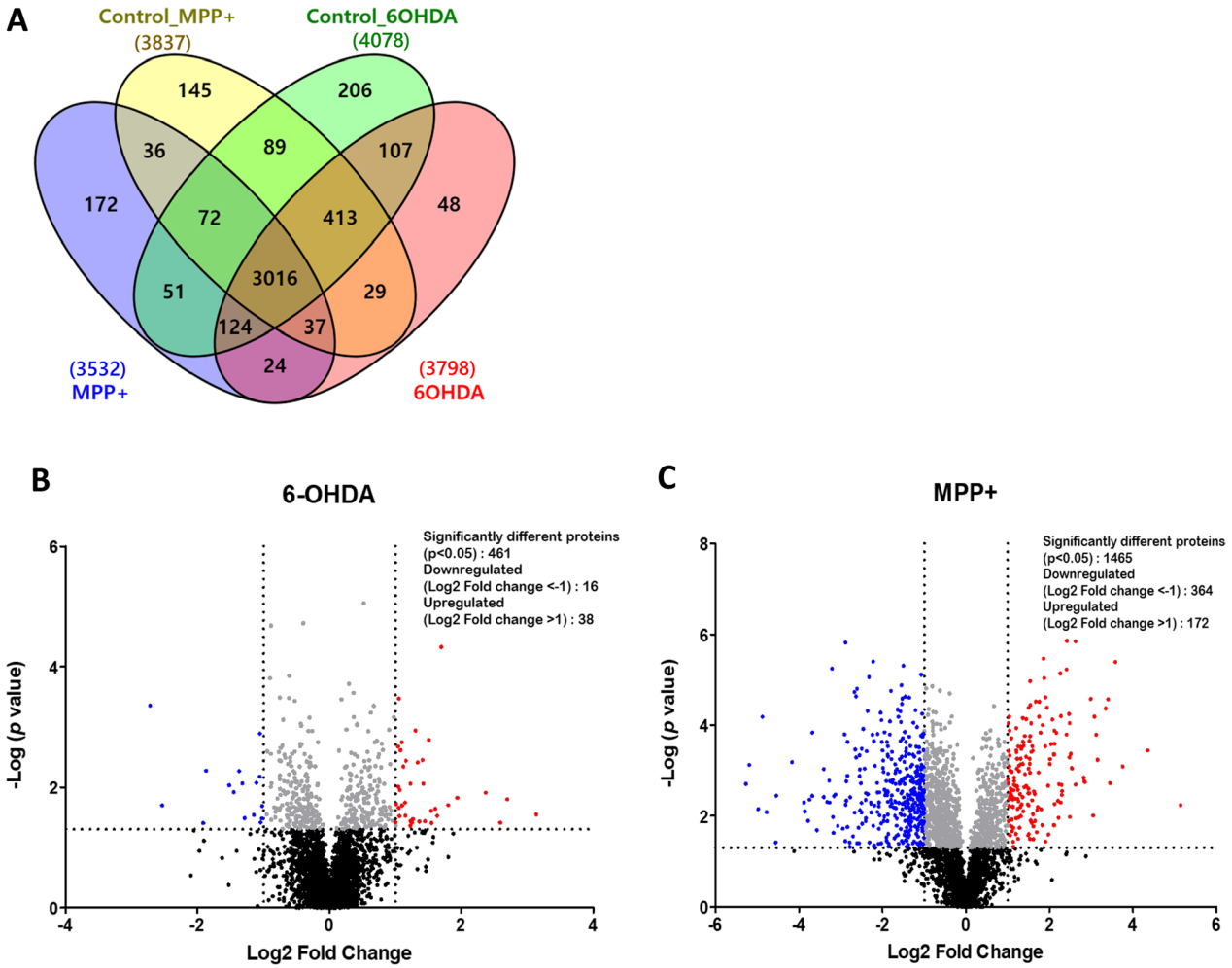

Fig. 2 A comprehensive overview of proteomics. **A** Venn diagram showing the number of identified proteins in each of the following four proteome sets: 6-OHDA control, 6-OHDA-treated, MPP+ control, and MPP+-treated. Volcano plot shows the differentially regulated proteins in **B** 6-OHDA-induced neurodegeneration in SH-SY5Y cells and **C** MPP+-induced neurodegeneration in SH-SY5Y cells. The horizontal coordinate (*X*-axis) represents the difference in fold change (logarithmic transformation at the base of 2), and the vertical coordinate (*Y*-axis) represents the significant difference in *p* value (logarithmic transformation at the base of 10). Proteins that are onefold significantly upregulated are presented as red dots, while those that are onefold downregulated are shown as blue dots. Proteins with a fold change less than onefold change are presented as gray dots. Black dots represent proteins that do not have a significant fold change. (For interpretation of the references to color in this figure legend, the reader is referred to the Web version of this article). *6-OHDA* 6-hydroxydopamine; *MPP+* 1-methyl-4-phenylpyridinium

bifunctional protein involved in the regulation and coordination of cell–cell adhesion and gene transcription (MacDonald et al. 2009). A recent study of PD-induced animal models confirmed a decrease in CTNNB1 expression (Marchetti et al. 2020), which confirmed a decrease in HMG-CoA synthesis-related proteins in PD (Durrenberger et al. 2012). In the case of MPP+, unlike 6-OHDA, mitochondrial dysfunction occurs owing to a decrease in HMG-CoA synthase protein expression, which induces neurodegeneration in SH-SY5Y cells. A comparative proteomics study of neurodegeneration in SH-SY5Y cells using 6-OHDA and MPP+ may provide further clues to explore the underlying causes of mitochondrial dysfunction in PD.

Comparative analysis of proteomes in SH-SY5Y cells showing neurodegeneration induced by 6-OHDA and MPP+

To verify whether 6-OHDA and MPP+ induce mitochondrial dysfunction via different mechanisms, a comparative analysis of 265 proteins showing significant differences in expression ($p < 0.05$) was conducted in 6-OHDA- and MPP+-treated SH-SY5Y cells. For a more accurate analysis, 100 proteins with more than

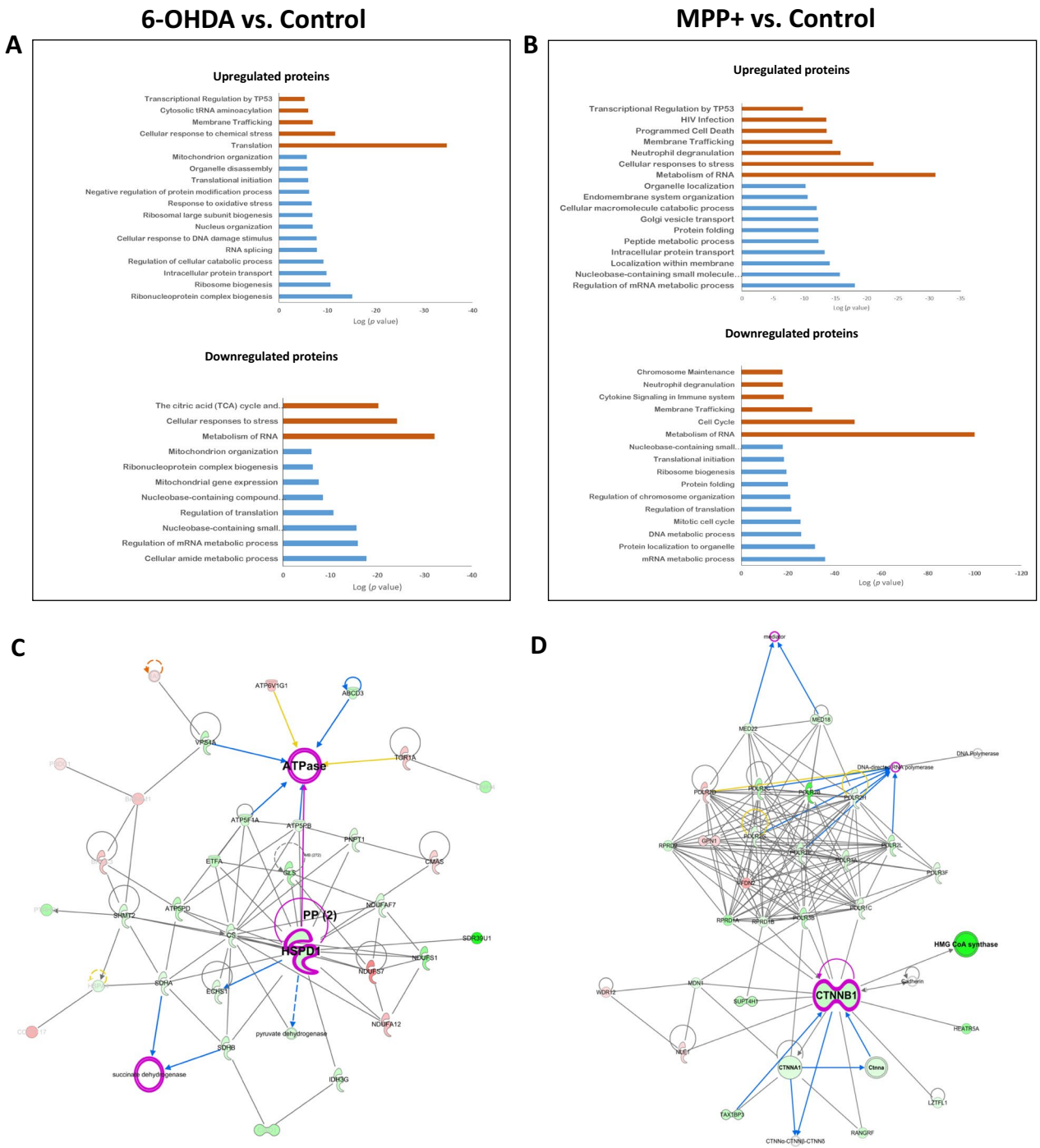

Fig. 3 Comparative analysis of the proteome of neurodegeneration induced by 6-OHDA or MPP+ in SH-SY5Y cells. The GO classification terms of biological process (blue bar), and reactome gene set analysis (orange bar) using Metascape online database on differentially expressed proteins ($p < 0.05$) in **A** 6-OHDA-treated SH-SY5Y cells compared with untreated SH-SY5Y cells and **B** MPP+-treated SH-SY5Y cells compared with untreated SH-SY5Y cells. Ingenuity pathway analysis of differentially expressed proteins ($p < 0.05$) after **C** 6-OHDA and **D** MPP+ treatment. Proteins are colored red (up) or green (down) based on fold-change values. (For interpretation of the references to color in this figure legend, the reader is referred to the Web version of this article). *6-OHDA* 6-hydroxydopamine, *MPP+* 1-methyl-4-phenylpyridinium

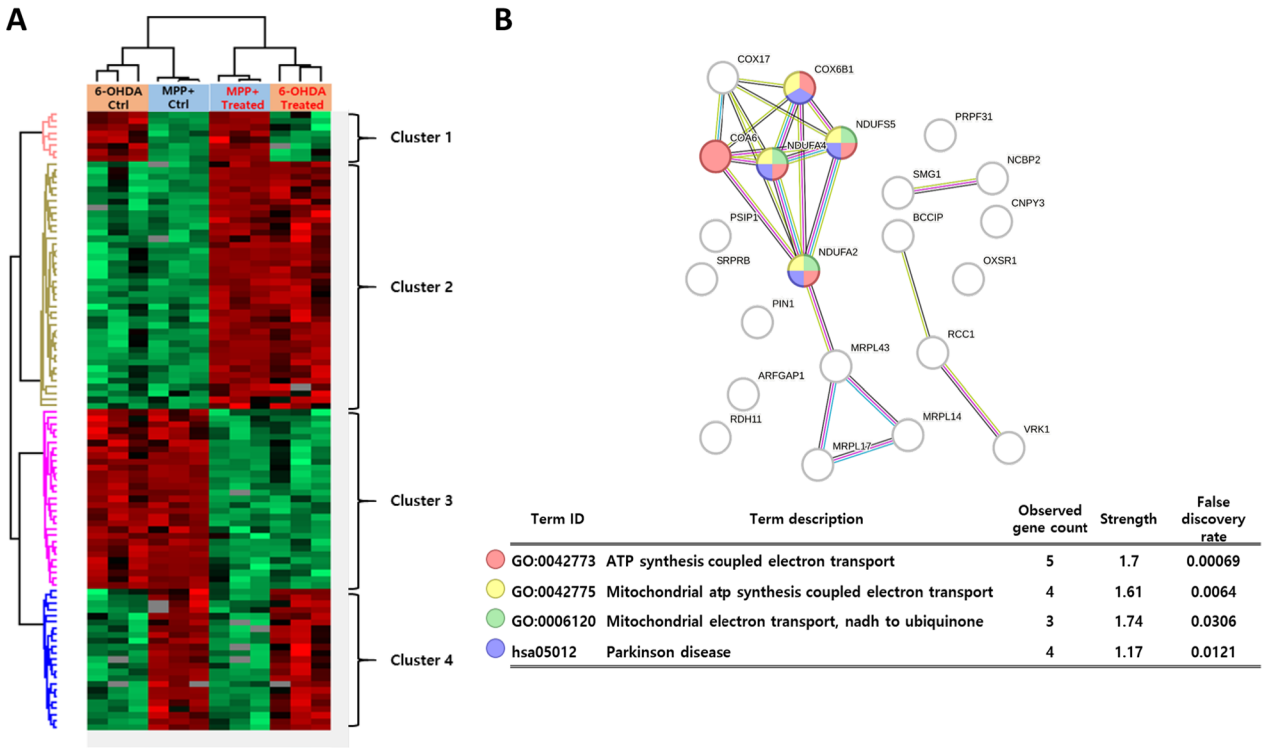

Term ID	Term description	Observed gene count	Strength	False discovery rate
GO:0042773	ATP synthesis coupled electron transport	5	1.7	0.00069
GO:0042775	Mitochondrial atp synthesis coupled electron transport	4	1.61	0.0064
GO:0006120	Mitochondrial electron transport, nadh to ubiquinone	3	1.74	0.0306
hsa05012	Parkinson disease	4	1.17	0.0121

Fig. 4. 6-OHDA and MPP+ reversibly altered the expression of electron transport proteins associated with mitochondrial dysfunction in SH-SY5Y cells. **A** Heatmap analysis of four conditions (6-OHDA control group, 6-OHDA treatment, MPP+ control group, and MPP+ treatment) for 100 proteins with $p < 0.05$ and fold change > 1.5 in 6-OHDA and MPP+-treated SH-SY5Y cells shows clusters enriched in each proteome set. **B** STRING protein–protein interaction analysis for 23 proteins represented by cluster 4 upregulated by 6-OHDA and downregulated by MPP+. *6-OHDA* 6-hydroxydopamine, *MPP+* 1-methyl-4-phenylpyridinium

1.5-fold changes in expression were selected for each of the 6-OHDA- and MPP+-treated SH-SY5Y cells among 265 proteins with significant differences. The hierarchical clustering heatmap of the 100 proteins is shown in Fig. 4A and is divided into four clusters. In Cluster 1, the expression of eight proteins was identified as downregulated in 6-OHDA-treated SH-SY5Y cells and upregulated in MPP+-treated SHY5Y cells compared to that in the control group. Most of them showed a strong correlation with the structural regulation, activity and binding of ribosomal proteins. Cluster 2 was identified as 40 upregulated proteins in both 6-OHDA- and MPP+-treated SH-SY5Y cells, and GO biological process analysis confirmed that the endoplasmic reticulum (ER)-targeting protein, SRP-dependent translational protein targeting the membrane, and cytoplasmic translation were strongly correlated. ER stress has been previously reported to cause neurodegenerative diseases (Lindholm et al. 2006), and recent studies have confirmed that ER-mitochondrion-associated homeostasis is an important factor in neurodegeneration (Gómez-Suaga et al. 2018). Cluster 3 was identified as 29 downregulated proteins in both 6-OHDA- and MPP+-treated cells, and GO biological process analysis confirmed that glutamine metabolism-related proteins were strongly correlated. Glutamate, which is produced by glutamine metabolism, is a precursor of GABA that functions as a neurotransmitter and is an important amino acid in neuronal interactions. Deficiency of glutamine metabolism proteins leads to deficiency of glutamate and degeneration of neurons, which can lead to the development of various neurological diseases besides PD (Wang et al. 2020). Finally, in Cluster 4, it was confirmed that the expression of 23 proteins were upregulated in 6-OHDA-treated SH-SY5Y cells and downregulated in MPP+-treated SHY5Y cells compared to that in the control group (Table 1). A recent study by Toomey et al. found differences in mitochondrial function-related protein expression in brain regions of PD patients, along with differences in electron transport-related proteins in mitochondrial function-related proteins between early and late PD patients (Toomey et al. 2022). Among the data we analyzed, GO analysis showed that the proteins in Cluster 4 were closely related to the mitochondrial electron transport system. Cluster 4 proteins in 6-OHDA-treated SH-SY5Y cells matched the expression of the mitochondrial electron transport

Table 1 List of 23 proteins represented by cluster 4 expression upregulated by 6-OHDA and downregulated by MPP+ in Fig. 4

UniProt accession	Protein description	Gene symbol	6-OHDA versus control		MPP+ versus control	
			Log2 fold change	*p* value	Log2 fold change	*p* value
Q13526	Peptidyl-prolyl cis–trans isomerase NIMA-interacting 1	PIN1	0.588	3.37E−02	−0.871	4.21E−02
H0Y6Y8	39S ribosomal protein L43, mitochondrial	MRPL43	1.120	4.57E−03	−1.659	1.14E−02
P52298	Nuclear cap-binding protein subunit 2	NCBP2	0.805	2.85E−02	−0.710	1.79E−02
Q9BT09	Protein canopy homolog 3	CNPY3	1.051	3.39E−04	−1.009	3.04E−02
J3KRA9	Serine/threonine-protein kinase SMG1	SMG1	0.650	2.74E−02	−2.869	4.63E−03
Q9Y2R5	28S ribosomal protein S17, mitochondrial	MRPS17	0.648	2.60E−02	−1.713	3.09E−02
O75475	PC4 and SFRS1-interacting protein	PSIP1	1.010	1.93E−02	−5.273	1.98E−03
Q9Y5M8	Signal recognition particle receptor subunit beta	SRPRB	0.761	8.17E−03	−1.112	2.01E−03
O43678	NADH dehydrogenase [ubiquinone] 1 alpha subcomplex subunit 2	NDUFA2	0.647	4.00E−02	−1.172	8.15E−04
Q14061	Cytochrome c oxidase copper chaperone	COX17	1.225	4.41E−02	−1.911	1.69E−03
Q8TC12	Retinol dehydrogenase 11	RDH11	0.638	4.35E−02	−1.457	1.50E−03
Q9NRX2	39S ribosomal protein L17, mitochondrial	MRPL17	2.367	1.23E−02	−2.084	5.06E−03
Q99986	Serine/threonine-protein kinase VRK1	VRK1	0.673	2.23E−02	−3.748	4.41E−03
Q9P287	BRCA2 and CDKN1A-interacting protein	BCCIP	0.686	7.90E−03	−0.810	1.39E−05
P18754	Regulator of chromosome condensation	RCC1	0.740	3.14E−03	−1.571	4.93E−05
O43920	NADH dehydrogenase [ubiquinone] iron–sulfur protein 5	NDUFS5	1.447	3.68E−02	−1.370	1.23E−02
Q6P1L8	39S ribosomal protein L14, mitochondrial	MRPL14	1.546	3.94E−02	−2.886	1.52E−06
O00483	Cytochrome c oxidase subunit NDUFA4	NDUFA4	1.423	8.74E−03	−2.612	1.57E−05
Q8WWY3	U4/U6 small nuclear ribonucleoprotein Prp31	PRPF31	0.611	4.62E−03	−0.718	2.88E−03
Q5JTJ3	Cytochrome c oxidase assembly factor 6 homolog	COA6	1.410	3.54E−03	−0.617	3.67E−02
O95747	Serine/threonine-protein kinase OSR1	OXSR1	0.735	1.17E−02	−0.619	1.04E−02
Q8N6T3	ADP-ribosylation factor GTPase-activating protein 1	ARFGAP1	0.587	1.18E−03	−1.546	9.55E−03
P14854	Cytochrome c oxidase subunit 6B1	COX6B1	1.696	4.71E−05	−2.884	5.69E−03

SH-SY5Y cells were treated with 50 μM 6-OHDA or 500 μM MPP+ for 48 h

6-OHDA 6-hydroxydopamine, *MPP+* 1-methyl-4-phenylpyridinium

system proteins in early PD patients, and in the case of MPP+-treated SH-SY5Y cells, the expression of mitochondrial electron transport system proteins was consistent with that observed in late PD patients. This suggests that SH-SY5Y cells treated with 6-OHDA can be used to mimic an early PD model, while MPP+-treated SH-SY5Y cells mimic the late PD model. This was also verified by PPI network analysis using STRING, where the electron transport-related proteins were confirmed to be relevant to PD (Fig. 4B). These results are consistent with the IPA results (Fig. 2C, D), which analyzed all the significant proteins described earlier. It was also confirmed in previous experiments that mitochondrial dysfunction was induced by electron transport system changes induced by 6-OHDA or MPP+ (Fig. 1F), such as mitochondrial dysfunction due to ER-mitochondrion-associated homeostasis loss in Cluster 2. Mitochondrial dysfunction causes apoptosis, and neuronal cell apoptosis induces the development of neurodegenerative diseases such as PD.

Conclusions

We validated a SH-SY5Y cell PD model via comparative proteomic analysis of the PD model cells induced by 6-OHDA and MPP+. Proteomic analysis of 6-OHDA- and MPP+-induced PD model cells revealed that protein changes in the electron transport system are critical for mitochondrial dysfunction and apoptosis. However, proteomic analysis revealed that two compounds, 6-OHDA and MPP+, reversibly altered the expression of electron transport proteins associated with mitochondrial dysfunction in SH-SY5Y cells. These results suggest that each of the two compounds, 6-OHDA and MPP+, may work in a different way on the electron transport system to cause mitochondrial dysfunction in SH-SY5Y cells. Our findings will aid in understanding the fundamental mechanisms of PD and provide new insights into the discovery of new treatment targets for the disease.

Abbreviations

PD	Parkinson's disease
6-OHDA	6-Hydroxydopamine
MPP+	1-Methyl-4-phenylpyridinium
DEPs	Differentially expressed proteins
LFQ	Label-free quantification
GO	Gene ontology
ER	Endoplasmic reticulum

Acknowledgements
We thank the laboratory members for their help in the study. We would like to thank Editage (www.editage.co.kr) for English language editing.

Author contributions
JYH, SHY, HJL, EHH, and YHC conceptualized and designed the study. JYH, SHY, and HJL performed the experiments. JYH drafted the manuscript. YHC guided the research and revised the manuscript. All authors have read and approved the final manuscript.

Funding
This research was supported by a National Research Foundation of Korea grant funded by the Korean Government (MSIT; 2022, R&D Equipment Engineer Education Program, 2014R1A6A9064166), a grant from the Korea Basic Science Institute (C270100) funded by the Ministry of Science and ICT, and the Establishment of Technology Commercialization Collaboration Platform through the Korea Innovation Foundation funded by the Ministry of Science and ICT (Establishing Project on the Collaboration Platform of the Technology Commercialization for Biomedical Industry in INNOPOLIS Daedeok, 1711149917).

Availability of data and materials
All data and materials are available on request.

Declarations

Competing interests
The authors declare that they have no competing interests.

Received: 10 November 2022 Accepted: 25 December 2022
Published online: 09 January 2023

References

Alberio T, Bondi H, Colombo F, Alloggio I, Pieroni L, Urbani A, Fasano M. Mitochondrial proteomics investigation of a cellular model of impaired dopamine homeostasis, an early step in Parkinson's disease pathogenesis. Mol Biosyst. 2014;10(6):1332–44.
Aslam B, Basit M, Nisar MA, Khurshid M, Rasool MH. Proteomics: technologies and their applications. J Chromatogr Sci. 2017;55:182–96.
Bence NF, Sampat RM, Kopito RR. Impairment of the ubiquitin-proteasome system by protein aggregation. Science. 2001;292:1552–5.
Bertin E, Chaté H, Ginelli F, Mishra S, Peshkov A, Ramaswamy S. Mesoscopic theory for fluctuating active nematics. New J Phys. 2013;15:085032.
Blum D, Torch S, Lambeng N, Nissou M, Benabid AL, Sadoul R, Verna JM. Molecular pathways involved in the neurotoxicity of 6-OHDA, dopamine and MPTP: contribution to the apoptotic theory in Parkinson's disease. Prog Neurobiol. 2001;65:135–72.
Chen Y, Song D, Chen C, Liu T, Cheng O. Dexmedetomidine protects SH-SY5Y cells against MPP+-induced declining of mitochondrial membrane potential and cell cycle deficits. Eur J Neurosci. 2021;54:4141–53.
Choi JW, Song MY, Park KS. Quantitative proteomic analysis reveals mitochondrial protein changes in MPP(+)-induced neuronal cells. Mol Biosyst. 2014;10(7):1940–7.
Cox J, Mann M. MaxQuant enables high peptide identification rates, individualized p.p.b.-range mass accuracies and proteome-wide protein quantification. Nat Biotechnol. 2008;26:1367.
Cox J, Neuhauser N, Michalski A, Scheltema RA, Olsen JV, Mann M. Andromeda: a peptide search engine integrated into the MaxQuant environment. J Proteome Res. 2011;10:1794.
Do Lee Y, Lee KS, Lee HJ, Noh YH, Do Kim H, Lee JY, et al. Kynurenic acid attenuates MPP(+)-induced dopaminergic neuronal cell death via a Bax-mediated mitochondrial pathway. Eur J Cell Biol. 2008;87:389–97.
Durrenberger PF, Grünblatt E, Fernando FS, Monoranu CM, Evans J, Riederer P, Reynolds R, Dexter DT. Inflammatory pathways in Parkinson's disease; A BNE microarray study. Parkinsons Dis. 2012;2012:214714.
Filograna R, Civiero L, Ferrari V, Codolo G, Greggio E, Bubacco L, Beltramini M, Bisaglia M, Castresana JS. Analysis of the catecholaminergic phenotype in human SH-SY5Y and BE(2)-M17 neuroblastoma cell lines upon differentiation. PLoS ONE. 2015;10:e0136769.
Ganapathy K, Datta I, Sowmithra S, Joshi P, Bhonde R. Influence of 6-hydroxydopamine toxicity on α-synuclein phosphorylation, resting vesicle expression, and vesicular dopamine release. J Cell Biochem. 2016;117(12):2719–36.
Gómez-Suaga P, Bravo-San Pedro JM, González-Polo RA, et al. ER–mitochondria signaling in Parkinson's disease. Cell Death Dis. 2018;9:337.
Hernandez SM, Tikhonova EB, Karamyshev AL. Protein–protein interactions in alpha-synuclein biogenesis: new potential targets in Parkinson's disease. Front Aging Neurosci. 2020;12:72.
Katsuyama M, Kimura E, Ibi M, Iwata K, Matsumoto M, Asaoka N, Yabe-Nishimura C. Clioquinol inhibits dopamine-β-hydroxylase secretion and noradrenaline synthesis by affecting the redox status of ATOX1 and copper transport in human neuroblastoma SH-SY5Y cells. Arch Toxicol. 2021;95:135–48.
Khwanraj K, Phruksaniyom C, Madlah S, Dharmasaroja P. Differential expression of tyrosine hydroxylase protein and apoptosis-related genes in differentiated and undifferentiated SH-SY5Y neuroblastoma cells treated with MPP+. Neurol Res Int. 2015;2015:734703.
Komatsubara AT, Asano T, Tsumoto H, et al. Proteomic analysis of S-nitrosylation induced by 1-methyl-4-phenylpyridinium (MPP+). Proteome Sci. 2012;10:74.
Kovalevich J, Langford D. Considerations for the use of SH-SY5Y neuroblastoma cells in neurobiology. Methods Mol Biol. 2013;1078:9–21.
Lee SY, Yun SH, Lee H, et al. Multi-omics analysis of aniline-degrading bacterium, *Delftia* sp. K82. J Anal Sci Technol. 2021a;12:6.
Lee JH, Hwang Y-J, Li H, Kim H, Suh M-W, Han D, Oh S-H. In-depth proteome of perilymph in guinea pig model. Proteomics. 2021b;21:e2000138.
Lindholm D, Wootz H, Korhonen L. ER stress and neurodegenerative diseases. Cell Death Differ. 2006;13:385–92.
MacDonald BT, Tamai K, He X. Wnt/beta-catenin signaling: components, mechanisms, and diseases. Dev Cell. 2009;17(1):9–26.
Magalingam KB, Somanath SD, Ramdas P, Haleagrahara N, Radhakrishnan AK. 6-Hydroxydopamine induces neurodegeneration in terminally differentiated SH-SY5Y neuroblastoma cells via enrichment of the nucleosomal degradation pathway: a global proteomics approach. J Mol Neurosci. 2022;72(5):1026–46.
Marchetti B, Tirolo C, L'Episcopo F, et al. Parkinson's disease, aging and adult neurogenesis: Wnt/β-catenin signalling as the key to unlock the mystery of endogenous brain repair. Aging Cell. 2020;19:e13101.
Muchowski PJ, Wacker JL. Modulation of neurodegeneration by molecular chaperones. Nat Rev Neurosci. 2005;6:11–22.
Perfeito R, Cunha-Oliveira T, Rego AC. Reprint of: revisiting oxidative stress and mitochondrial dysfunction in the pathogenesis of Parkinson disease-resemblance to the effect of amphetamine drugs of abuse. Free Radic Biol Med. 2013;62:186–201.
Ross OA, Braithwaite AT, Skipper LM, Kachergus J, Hulihan MM, et al. Genomic investigation of alpha-synuclein multiplication and parkinsonism. Ann Neurol. 2008;63:743–50.
Smith WW, Pei Z, Jiang H, Moore DJ, Liang Y, West AB, Dawson VL, Dawson TM, Ross CA. Leucine-rich repeat kinase 2 (LRRK2) interacts with parkin, and mutant LRRK2 induces neuronal degeneration. Proc Natl Acad Sci USA. 2005;102(51):18676–81. https://doi.org/10.1073/pnas.0508052102.
Toomey CE, Heywood WE, Evans JR, et al. Mitochondrial dysfunction is a key pathological driver of early stage Parkinson's. Acta Neuropathol Commun. 2022;10(1):134. https://doi.org/10.1186/s40478-022-01424-6.
Tsang AH, Chung KK. Oxidative and nitrosative stress in Parkinson's disease. Biochim Biophys Acta. 2009;1792:643–50.

Tusher VG, Tibshirani R, Chu G. Significance analysis of microarrays applied to the ionizing radiation response. Proc Natl Acad Sci USA. 2001;98:5116–21.
Tyanova S, Temu T, Sinitcyn P, Carlson A, Hein MY, Geiger T, Mann M, Cox J. The Perseus computational platform for comprehensive analysis of (prote) omics data. Nat Methods. 2016;13:731.
Välikangas T, Suomi T, Elo LL. A comprehensive evaluation of popular proteomics software workflows for label-free proteome quantification and imputation. Brief Bioinform. 2018;19(6):1344–55.
Wang J, Song W. Regulation of LRRK2 promoter activity and gene expression by Sp1. Mol Brain. 2016;22(9):33.
Wang F, Awan UF, Wang Y, Wang L, Qing H, Ma H, Deng Y. Damage of neuroblastoma cell SH-SY5Y mediated by MPP^+ inhibits proliferation of T-cell leukemia jurkat by co-culture system. Int J Mol Sci. 2014;15:10738–50.
Wang J, Li Y, Gao L, Yan F, Gao G, Li L. GSK-3β inhibitor alsterpaullone attenuates MPP^+-induced cell damage in a c-Myc-dependent manner in SH-SY5Y cells. Front Cell Neurosci. 2018;12:283.
Wang J, Wang F, Mai D, Qu S. Molecular mechanisms of glutamate toxicity in Parkinson's disease. Front Neurosci. 2020;14:585584.
Xie H, Chang M, Hu X, Wang D, Tian M, Li G, Jiang H, Wang Y, Dong Z, Zhang Y, Hu L. Proteomics analysis of MPP+-induced apoptosis in SH-SY5Y cells. Neurol Sci. 2011;32(2):221–8.
Zhang N, Shu H-Y, Huang T, Zhang Q-L, Li D, Zhang G-Q, et al. Nrf2 signaling contributes to the neuroprotective effects of urate against 6-OHDA toxicity. PLoS ONE. 2014;9(6):e100286.
Zhou Y, Zhou B, Pache L, Chang M, Khodabakhshi AH, Tanaseichuk O, Benner C, Chanda SK. Metascape provides a biologist-oriented resource for the analysis of systems-level datasets. Nat Commun. 2019;10(1):1523.

Publisher's Note